Protist 174 (2023) 125992

Contents lists available at ScienceDirect

Protist

journal homepage: www.elsevier.de/protis

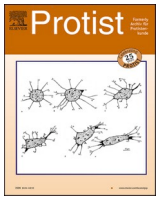

Genomic architecture constrains macromolecular allocation in dinoflagellates

Olga Carnicer [a], Ying-Yu Hu [a], Vinitha Ebenezer [a], Andrew J. Irwin [b], Zoe V. Finkel [a,*]

[a] Department of Oceanography, Dalhousie University, Halifax, Canada
[b] Department of Mathematics & Statistics, Dalhousie University, Halifax, Canada

ARTICLE INFO

Monitoring Editor: Laure Guillou

Key words:
dinoflagellate
elemental stoichiometry
macromolecules
DNA content
genome size
RNA: protein

Dinoflagellate genomes have a unique architecture that may constrain their physiological and biochemical responsiveness to environmental stressors. Here we quantified how nitrogen (N) starvation influenced macromolecular allocation and C:N:P of three photosynthetic marine dinoflagellates, representing different taxonomic classes and genome sizes. Dinoflagellates respond to nitrogen starvation by decreasing cellular nitrogen, protein and RNA content, but unlike many other eukaryotic phytoplankton examined RNA:protein is invariant. Additionally, 2 of the 3 species exhibit increases in cellular phosphorus and very little change in cellular carbon with N-starvation. As a consequence, N starvation induces moderate increases in C:N, but extreme decreases in N:P and C:P, relative to diatoms. Dinoflagellate DNA content relative to total C, N and P is much higher than similar sized diatoms, but similar to very small photosynthetic picoeukaryotes such as *Ostreococcus*. In aggregate these results indicate the accumulation of phosphate stores may be an important strategy employed by dinoflagellates to meet P requirements associated with the maintenance and replication of their large genomes.

1. Introduction

Dinoflagellates are diverse group of eukaryotic protists, with approximately 2400 named species, that includes photosynthetic, mixotrophic and heterotrophic members, with cell diameters ranging from <5 to many 100s of microns (Gómez 2012; Lin 2006). Dinoflagellates are common and often abundant members of both freshwater and marine plankton communities, that often form blooms (Hallegraeff 1993; Smayda and Reynolds 2003). Relative to diatoms that tend to bloom in cooler, more nitrate-rich environments with deeper mixed layers, dinoflagellates often bloom in more stratified, warmer and more nutrient-poor conditions (Irwin et al. 2012; Smayda and Reynolds 2003). There is some evidence that climate warming may increase the relative abundance of dinoflagellates within plankton communities and the frequency of dinoflagellate blooms, some of which may be toxic (Hallegraeff 1993; Leterme et al. 2005). An increase in harmful dinoflagellate blooms can have significant economic consequences (Anderson and Garrison 1997; Shumway 1990).

Dinoflagellates are defined by a number of noteworthy cellular and biochemical characters. As alveolates they have flattened vesicles under the plasma membrane that can contain thick carbon-rich cellulosic plates. Species with conspicuous plates are referred to as thecate, and those with missing or thin plates as athecate (Hoppenrath 2017). Thecate species are often higher in total particulate organic carbon relative to organic nitrogen content than athecate species and other phytoplankton groups such as diatoms (Carnicer et al. 2021; Menden-Deuer and Lessard 2000). Dinoflagellates exhibit an enormous range of genome sizes and unusual genetic architecture (Hackett and Bhattacharya 2006). Nucleic acids are relatively rich in organic P (Geider and LaRoche 2002), and therefore larger genomes may result in lower total cellular N:P compared to other eukaryotic microbes (Carnicer et al. 2021). Shifts in planktonic community composition from the siliceous-walled diatoms relative to dinoflagellates with higher C:N and lower N:P could have significant consequences for both food web structure and function and the biogeochemical cycling of carbon and other bio-limiting elements (Deutsch and Weber 2012; Sterner and Elser 2002; Williams and Follows 2011). A characterization of the macromolecular and cellular determinants of C:N:P in dinoflagellates is required to improve our understanding of their niche, how they are likely to respond to environmental changes and their impact on the biogeochemical cycling of C, N and P.

Dinoflagellate genomes are characterized by a number of unusual features that may influence both their nutrient requirements and ability to respond to environmental stressors. Dinoflagellate DNA content ranges from 1.5 to >250 pg (Hong et al. 2016; LaJeunesse et al. 2005); genomes larger that 20 pg are atypical for eukaryotes (Hidalgo et al.

* Corresponding author at: Department of Oceanography, Dalhousie University, Halifax, NS Canada.
E-mail address: zfinkel@dal.ca (Z.V. Finkel).

https://doi.org/10.1016/j.protis.2023.125992
Received 13 April 2023; Accepted 11 September 2023
Available online 12 September 2023

2017). Hydroxymethyluracil can replace up to 60% of the thymine in DNA (Herzog et al. 1982; Rae 1976). Dinoflagellate nuclei are low in histone and total protein content (Rizzo 2003; Rizzo and Nooden 1973). Most dinoflagellates lack nucleosomal structure and their chromosomes are permanently condensed (Spector 1984). It is hypothesized that dinoflagellate DNA has a chlorestic liquid crystal structure with stacked sheets of parallel DNA filaments (Livolant and Bouligand 1978) that may influence transcription (Marinov et al. 2021). Dinoflagellate genes are organized in large gene families in tandem arrays, and transcripts are polycistronic (H. Zhang et al. 2007, 2009), but see Beauchemin et al. (2012). There is some indication that dinoflagellates may have relatively limited transcriptional regulation (Lin 2011; Ou et al. 2019). The unusual genetic architecture and large genome size of dinoflagellates may impact their macromolecular (for example: DNA:RNA:protein) and elemental (C:N:P) stoichiometry and their ability to respond to nutrient stress and starvation and other environmental perturbations. It is hypothesized that organisms with large genome sizes, such as many dinoflagellates, will have higher nitrogen and phosphorus requirements for growth and division and that the genome size and structure may limit transcriptional and biochemical capacities to respond to environmental stressors (Hessen et al. 2010; Hidalgo et al. 2017).

Here we quantify the elemental (C, N and P) and macromolecular composition (including DNA, RNA, protein, carbohydrate, lipid, phospholipid and polyphosphate content) of three marine photosynthetic dinoflagellates species representing three different taxonomic orders under both nutrient-sufficient and nitrogen-starvation conditions to determine if the high DNA content of dinoflagellates influences cellular nitrogen and phosphorus content and macromolecular reallocation strategies in response to nitrogen starvation. We find that dinoflagellate DNA content relative to C, N or P is considerably higher than similar-sized diatoms but is comparable to small photosynthetic picoeukaryotes such as *Ostreococcus*. In response to nitrogen starvation, like other phytoplankton groups, dinoflagellates exhibit decreases in protein and PON content, but in contrast to other taxonomic groups examined RNA: protein is invariant, and cellular phosphorus increases in some species, resulting in large decreases in total particulate N:P under nitrogen starvation. These results indicate dinoflagellates have a unique biochemical response to nitrogen starvation and that phosphate storage may be especially important for the survival and success of organisms that have large genomes and are subject to nutrient limitation.

2. Methods

2.1. Species and culture conditions

Three marine photosynthetic dinoflagellates were chosen to represent a range of taxonomic orders, cell sizes and wall types. The dinoflagellate species *Levanderina fissa* (Levander) Moestrup et al., 2014 (Gymnodiniales, thecate) CCMP2935, *Prorocentrum triestinum* J.Schiller, 1918 (Prorocentrales, athecate) CCMP700, and *Alexandrium minutum* Halim, 1960 (Gonyaulacales, athecate) IRTA-SMM-16-017 were maintained in modified f/2 media (900 μM sodium nitrate, 20–25 μM phosphate) with an aged (4 months) seawater base obtained from Station 2 on the Halifax line (c. 30 km offshore). *L. fissa* and *P. triestinum* were provided by Roscoff Culture Collection and isolated from the mid-latitude North Atlantic; *A. minutum* was provided by the Institute of Agrifood Research and Technology (IRTA) and isolated from the Mediterranean Sea. All the strains were maintained in exponential growth by serial dilution under an irradiance of 100 μmol photons m^{-2} s^{-1} with a 12 h: 12 h light: dark cycle, temperature of 20.5 °C, and manually shaken twice daily. *L. fissa* was cultured in 5 L glass bottles with a salinity of 30 psu; *P. triestinum* and *A. minutum* were cultured in 2 L plastic bottles with a salinity of 32 psu. Cultures were maintained in exponential growth for at least 10 generations with a constant exponential growth (re-inoculated every three to four days) prior to sampling and initiating the N-starvation experiment. To reduce bacterial contamination during acclimation prior to the experiment, cells were filtered through PC filters (10 μm pore size for *L. fissa* and 3 μm for *P. triestinum* and *A. minutum*). Filters were resuspended in new media treated with antibiotics. A stock of antibiotics was prepared, 100 μg mL^{-1} of streptomycin (Sigma) and 20 μg mL^{-1} of gentamycin (Sigma), with filtered Milli-Q water and stored at −20 °C.

2.2. Nitrogen starvation experiment

Nutrient-replete exponentially-growing dinoflagellate cultures in triplicate bottles were sampled for inorganic nitrogen and phosphate concentration, cell counts, cell volume, photophysiology, and elemental and macromolecular composition at either 2 or 3 days after dilution with modified nutrient-replete f/2 media (the nutrient-replete control samples, often referred to as t = 0). The nitrogen starvation treatment was created by either centrifuging or filtering nutrient-replete exponentially growing cell cultures and resuspending cells into media with no added nitrogen. For *L. fissa* the culture was centrifuged at ~100 g for 4 min, the pellets were transferred to triplicate 5 L bottles for each N-starvation sampling day with the modified f/2 media with no added nitrogen, resulting in a final cell density of 650 to 700 cells mL^{-1}. These bottles were then sampled at 4 different days (between days 2 to 13) after the initiation of the N-starvation treatment for inorganic nitrogen and phosphate concentration, cell counts, cell volume, photophysiology, and elemental and macromolecular composition. For *A. minutum* and *P. triestinum*, exponentially growing nutrient-sufficient cells were collected onto 47 mm, 3 μm pore size polycarbonate filters and then transferred into twelve 2 L bottles with modified f/2 media with no added nitrogen at cell densities of approximately 4100 and 6400 cells mL^{-1}, respectively. Three replicate bottles were sampled at 3, 5, 7, and 9 days for *A. minutum*, and *P. triestinum* was sampled at 2, 4, 9 and 13 days, after the initiation of the N-starvation treatment. The pH of the medium was monitored with a VWR sympHony benchtop meter on sampling days.

2.3. Cell counts and growth rate

Samples were taken, in triplicate, from each triplicate bottle for estimates of cell density and cell volume. Lugol's solution was added to these samples and then they were stored at 6 °C until analysis. Counts were made using a Sedgewick Rafter (1 mL) chamber and light microscope (Leica DN 4500) under 200X final magnification. Maximum growth rate (μ_{max}, d^{-1}) was calculated for the nutrient-replete exponentially acclimated cultures. There was a small lag phase immediately after the serial dilution, so the first cell count after dilution was not used in the calculation of μ_{max}. The decline in cell division rate over the nitrogen starvation experiment was determined from a two point difference in ln cell count between sampling days.

The mean cell volume of the dinoflagellate species were estimated from the nutrient-replete exponential growth conditions (t = 0) and after 9 days in nitrogen-deplete media (t = 9) assuming they were ellipsoid in shape. The length and width of individual cells were sized using a Zeiss Axioscope with camera and ImageJ calibrated with micrometer. A total of 70 individual cells were sized from 2 replicate bottles for *L. fissa*, 140 individuals from 4 replicate bottles for *P. triestinum* and 141 individuals from 4 replicate bottles for *A. minutum*, for each treatment.

2.4. Nutrient, elemental, chlorophyll-a and photophysiology analyses

Dissolved nitrite plus nitrate and phosphate were measured on sampling days from media or cultures filtered through a precombusted (4 h at 450 °C) GF/F filter using a Thermo Scientific 42iQ NO–NO 2–NOx Analyzer and a SEAL AutoAnalyzer 3 HR following the phosphomolybdate method specified by the manufacturer, respectively. Dissolved nutrient samples were stored in the freezer at −20 °C until analysis.

Samples for particulate carbon (C), nitrogen (N), and phosphorus (P) were collected on precombusted GF/F filters and stored in the freezer at −20 °C until analysis. For particulate carbon and nitrogen analyses, culture biomass and blanks were dried at 60 °C for 2 d, pelleted in pressed tin capsules, and analyzed with a UNICUBE Vario MICRO cube elemental analyzer. To differentiate between intracellular (IP) and extracellularly adsorbed phosphorus, two samples were taken, one rinsed with unenriched artificial seawater base to provide an estimate of total particulate phosphorus (TPP) and the other with an oxalate reagent (Tovar-Sanchez et al. 2003) to remove surface adsorbed P and provide an estimate of cellular phosphorus. For TPP and IP analyses, both types of samples were dried with 200 μL 0.17 M $MgSO_4$, combusted at 500 °C for 6 h and then digested by 0.2 M HCl at 90 °C for 30 min (Solórzano and Sharp 1980). Phosphorus was quantified using an ammonium molybdate method, modified for a microplate reader (Varioskan LUX multimode), using KH_2PO4 as a standard following (Hu, Irwin, et al. 2022).

Chlorophyll-*a* samples were collected on GF/F filters and stored at −20 °C until analysis. The samples were extracted directly by acetone: DMSO = 3:2 solvent for 30 min in the dark, in which acetone is 90% (v/v) of a saturated magnesium carbonate solution. Chlorophyll-*a* values were measured by a Turner Designs fluorometer (10-AU).

The dark-acclimated photochemical efficiency of PSII (Fv:Fm) was measured with a fluorescence induction and relaxation system (FIRe, Satlantic) using a gain of 850 to 950 and 40 acquisitions. Samples were taken every day in the middle of the light period following 5 min of dark acclimation.

2.5. Macromolecular sampling and analyses

Samples for carbohydrate and lipid were collected on pre-combusted 47 mm GF/F filters, while samples for protein, RNA, and DNA were collected on 0.6 μm (for *A. minutum* and *P. triestinum*) or 3 μm (for *L. fissa*) pore 47 mm polycarbonate membrane filters. Samples for macromolecular analyses were immediately placed in liquid nitrogen and then stored at −80 °C until analysis. Prior to analysis, all the samples were freeze-dried for approximately 2 h (FreeZone 2.5 L 50 C Benchtop Freeze Dryers, LABCONCO).

2.6. Protein

The detailed protocols for the estimate of crude and precipitated protein are available at protocols.io (Hu, Lord, et al. 2022b, 2022a). In brief, protein samples were homogenised in Lysing Matrix D tubes and extracted by protein extraction buffer (Ni et al. 2017). Bead milling was performed four times for 1 min at 6.5 m s^{-1} using a FastPrep-24 5G (MP Biomedicals), with samples placed on ice for 1 min between each round of bead milling to prevent degradation by heating. Extracted crude protein was then quantified using the BCA Assay and microplate reader (Varioskan LUX), with bovine serum albumin (BSA) used as a standard. The crude protein was subsequently precipitated by the chloroform–methanol method and dried in a vacuum desiccator. Precipitated protein was then redissolved in 95 μL Tris buffer (pH 8.0) with 5 μL 20% sarcosine, and measured using a BCA assay with a BSA standard.

2.7. RNA and DNA

The nucleic acid estimation method used is a modified version of Berdalet et al. (2005). DNA and RNA samples were placed in Lysing Matrix D tubes using an extraction buffer that included a 20% n-lauryl sarcosine sodium salt solution (Sigma-Aldrich L744), 5 mM Tris (pH 8.0, diluted from 1 M Tris, Fisher AAJ60080AK) and 0.5 mM EDTA (Bioshop EDT333.100). A FastPrep-24 5G (MP Biomedicals) unit was used to homogenize samples by four rounds of bead milling for 30 s at 6.5 m s^{-1}, with samples placed on ice for 1.5 min between each round of bead milling. The homogenate was then vortexed at room temperature for 1 h and then centrifuged (Eppendorf Centrifuge 5424 R) at 12,000 rpm for 5 min. The supernatant was treated with RNase (Sigma-Aldrich R6513), DNase (Bioshop DRB002.10), and RNase + DNase, and stained with SYBR Green II (Thermo Fisher S7564). RNA and DNA content were then determined by SYBR Green II fluorescence, with corrections applied based on the background fluorescence present after nuclease treatment. RNA was quantified against an *E. coli* ribosomal RNA standard (Ambion #7940) and DNA was quantified against a type IX calf thymus DNA standard (Sigma# D4522). RNA and DNA fluorescence were measured in a 96-well opaque black microplate.

2.8. Carbohydrate, lipid and phosphorus associated with the lipid fraction

Carbohydrate, lipids, and the phosphorus content in the lipid fraction (lipid-P) were all measured from the same sample filter. Samples were first vortexed in 9 M H_2SO_4 for 15 s and then diluted to a final H_2SO_4 molarity of 1.6 M and hydrolyzed for 3 h at 90 °C. Chloroform (2 mL) was added into the hydrolysate and then the mixture was centrifuged at 3200 rpm for 5 min at room temperature. The supernatant was transferred and then alkalinized by adding 12 M NaOH to the hydrolysate, the ratio of $[H^+]$ from the hydrolysate to $[OH^-]$ from NaOH was 0.82. Carbohydrate was measured using the alkalinized hydrolysate and a modified version of the TPTZ (2,4,6-Tri(2-pyridyl)-s-triazine) method (Myklestad et al. 1997) using 595 nm in microtiter plate and glucose as the standard. Methanol (1 mL) was added to the residue from the carbohydrate hydrolysis, vortexed and sonicated to extract lipids into the organic phase (Hu and Finkel 2022c, 2022b). A 0.88% KCl solution was added to the organic layer followed by a vortexing and then centrifuging at 3200 rpm for 5 min at room temperature. The lower organic phase was transferred to a storage vial, and the extract was dried under a stream of N_2 gas (<2 psi). The dried extract was redissolved using 5 mL of chloroform, and divided into two portions. Each portion was dried under a stream of N_2 gas. One portion was measured by acid–dichromate method (Pande et al. 1963) in a microtiter plate, absorbance was read at 348 nm instead of commonly used 440 nm for a much higher sensitivity and glyceryl tripalmitate (GTP) was used as standard (Hu and Finkel 2022a). The other portion was dried with 200 μL 0.17 M $MgSO_4$ and then combusted at 650 °C for 9 h. The ash was digested by 0.5 mL 0.2 M HCl at 90 °C for 30 min. The phosphate was then quantified using the ammonium molybdate method (Chen et al. 1956), modified for a microplate reader (Varioskan LUX multimode), using KH_2PO_4 as standard. The final phosphorus was corrected by a factor of 0.8 due to the incomplete recovery of phospholipids combusted at 650 °C (Hu, Irwin, et al. 2022).

2.9. Computations and statistical analyses

The C, N and P content (mol $cell^{-1}$) attributable to each macromolecular pool was calculated using the average stoichiometry for each macromolecule reported by Geider and Laroche (2002). Ratios were averaged using the geometric mean (exponential of the arithmetic mean of the log ratio.) Uncertainties in ratios were reported as 95% confidence intervals computed using bootstrap resampling on the log-transformed ratios. Elemental and macromolecular ratios were compared across taxa from this study plus *Ostreococcus tauri*, *Thalassiosira pseudonana*, and *Thalassiosira weisflogii* reported in Liefer et al. (2019). Ratios for exponentially-growing cultures were scaled so that the median across cultures was 1 for each ratio to highlight the variability and ranking of each ratio across taxa. Ratios for N-starved cultures (day 9 for the dinoflagellates and days 10 or 11 for *Ostreococcus* and the the diatoms) were divided by the ratio in exponential growth for each culture to highlight the variation between N-starved and replete conditions and enable comparisons across taxa. All analyses were performed using R version 4.1.3.

3. Results

A summary of all data showing averages, standard deviations, and sample sizes is provided in Table S1. The raw data with replication are reported in Dataset S1.

3.1. Cell division rate, and photophysiological response (Fv:Fm) to nitrogen starvation

The maximum resource-saturated exponential growth rate varied almost 2-fold, from 0.34 ± 0.01 d^{-1} for *A. minutum*, 0.34 ± 0.05 d^{-1} for *L. fissa*, and 0.67 ± 0.02 d^{-1} for *P. triestinum* (Fig. S1, mean ± 1 standard error, n = 3 or 4). For all the species examined, nitrate plus nitrate in the growth medium declined to concentrations below our detection limit 2 to 3 days after the initiation of the nitrogen-starvation treatment, and phosphate concentrations remained high (average > 18 µM) throughout the experiment (Fig. S1). Cell division rate ceased by the 4th day after transfer into nitrogen-free media for *P. triestinum*, day 6 for *L. fissa* and day 7 for the growing *A. minutum*. There was no consistent directional change in pH with N-starvation, and the changes were less than 0.3 pH units over the course of the N-starvation treatment (data not shown). Fv:Fm was highest under resource saturated conditions and declined with N-starvation (Fig. S1).

3.2. Cell volume and particulate carbon, nitrogen and phosphorus content

Cell volume was estimated from preserved samples under resource-saturated exponential growth conditions and after 9 days in the N-starvation treatment (Table S2). Cell volumes ranged from 1815 to 25767 μm^3 across the species; *P. triestinum* is the smallest and *L. fissa* the largest of the species examined. *A. minutum* and *L. fissa* decreased while *P. triestinum* increased in cell volume with N-starvation (Table S2). Cellular total particulate C, N and P increases with cell volume across species, but maximum resource replete growth rate does not (Table S1, Fig. S1). Under resource-saturated growth POC varies over an order of magnitude between small-sized *P. triestinum* (20.1 ± 0.9 pmol $cell^{-1}$, mean ± 1 sd) and the much larger *L. fissa* (246 ± 22 pmol $cell^{-1}$). Nitrogen starvation induces a > 2-fold decrease in cellular nitrogen in all three species, and a species-specific 1.5 to 3.3-fold increase in total particulate phosphorus (TPP) in *A. minutum* and *P. triestinum*, respectively, and no consistent change in TPP in *L. fissa* (Fig. 2, Table S1). The response of POC to N-starvation is inconsistent across species: increasing 2.3-fold in *P. triestinum*, oscillating over time with no net change by day 9 in *L. fissa*, and no change in *A. minutum* (Fig. 1). Decoupling between cell carbon and cell volume due to N-starvation has been reported for a number of dinoflagellates (Eker-Develi et al. 2006; Qi et al. 2013), due in some cases to changes in vacuolation or carbon accumulation associated with thecal plates (Béchemin et al. 1999; Flynn et al. 1996; John and Flynn 2000).

3.3. C:N:P

Under resource-saturated exponential growth C:N (mol:mol) varies from 7.5 in *P. triestinum* to 9.9 in *L. fissa*, N:IP from 7.5 in *A. minutum* to 11 in *L. fissa*, and C:IP from 60 in *A. minutum* to 108 in *L. fissa* (Fig. 1, see Table S2 for 95% CI on the ratios). In all the species examined, N-starvation causes an increase in C:N, but the increase is largest in *P. triestinum* due to its relatively larger increase in POC. The combined effect of the decrease in N quota and large increase in IP and TPP quota in *A. minutum* and *P. triestinum* with N-starvation results in large decreases in N:P (N:IP and N:TPP) with N-starvation in all three species examined. The ratio of intracellular to total phosphorus varies across the species with little to no change with N-starvation (Fig. 1, Table S2).

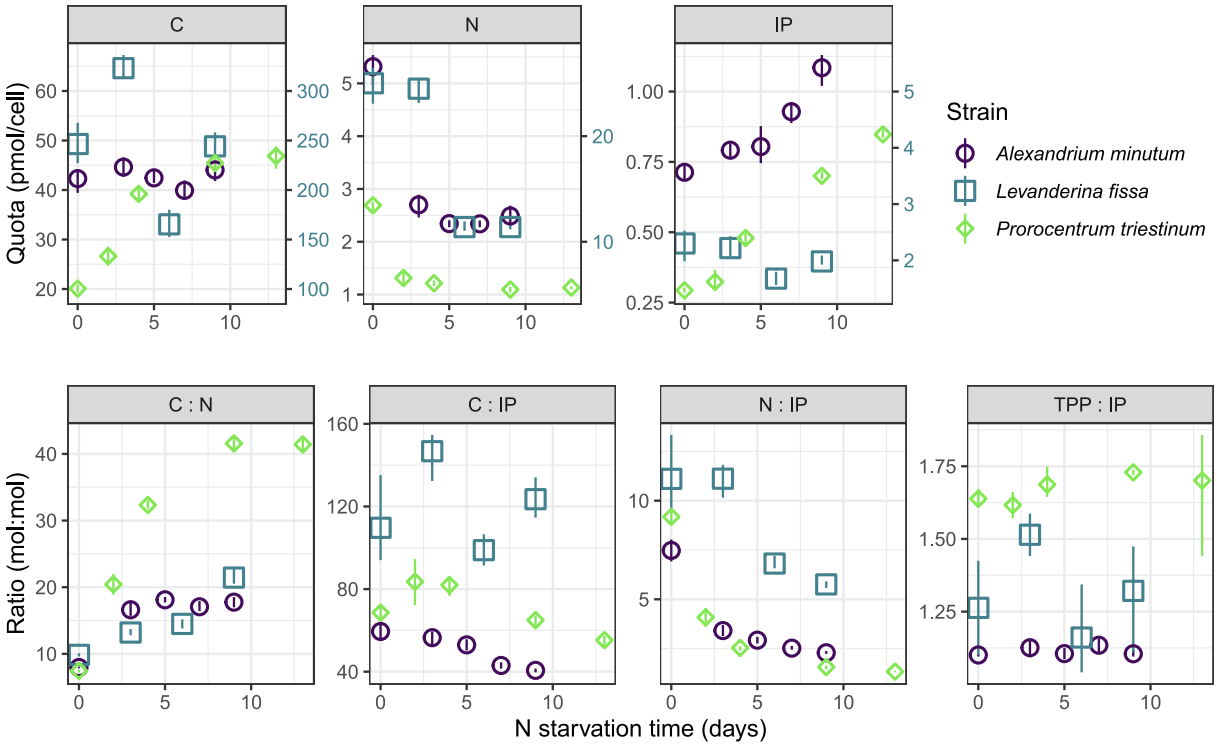

Fig. 1. Carbon (C), nitrogen (N), and intracellular particulate phosphorus (IP) cell quotas (pmol $cell^{-1}$) and ratios (mol:mol) for the three dinoflagellate taxa for nutrient-replete exponentially-growing cultures (t = 0) and nitrogen-starved cultures (t > 0 d). The last panel shows the total particulate phosphate (TPP, no oxalate rinse): intracellular particulate phosphate (IP, oxalate rinse). Sample size n = 4 biological replicates with two technical replicates for most bottles. Error bars are bootstrapped 95% confidence intervals on the mean (quotas) and geometric mean (ratios).

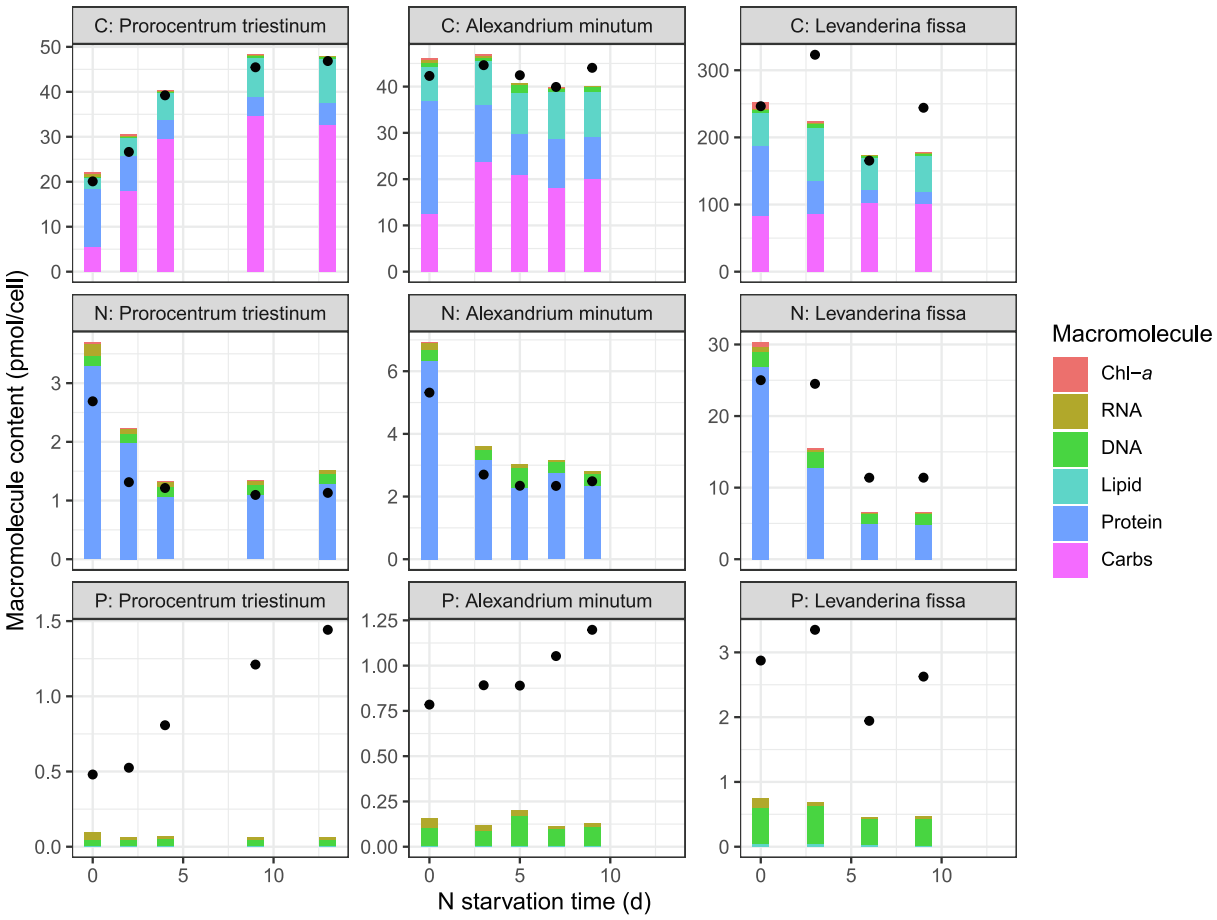

Fig. 2. Macromolecular (chlorophyll-*a*, RNA, DNA, lipid, crude protein, and carbohydrate (carbs)) decomposition of total cellular C, N, and TPP (pmol cell^{-1}) for three taxa under nutrient-replete exponentially-growing (t = 0) and nitrogen-starved conditions (t > 0 d). Contribution of macromolecule content (bars) to C (top row), N (middle row) or P (bottom row) and intracellular elemental quota (black points).

3.4. Macromolecular composition

Carbohydrate, lipid, protein, RNA, and DNA account for the majority of the particulate C and N in dinoflagellates. Most of cellular POC is in a combination of carbohydrate, protein and lipid, most of PON is protein with a smaller contribution from RNA, DNA and pigments such as chlorophyll-*a*. Cellular DNA and RNA account for less than 50% of total and cellular P (Fig. 2). In all species, nitrogen starvation results in a cellular decrease in protein, chlorophyll-*a* and RNA, while DNA is constant, and unaccounted for phosphorus increases (except for *L. fissa*). There are species-specific differences in carbohydrate and lipid content, with little change in either of these C-rich macromolecules with nitrogen starvation in *L. fissa*, a small increase in carbohydrate in *A. minutum*, and significant accumulation of both lipid and especially carbohydrate in *P. triestinum*. Chlorophyll-*a* is also quite variable across species: POC:chl-a (mass ratio) under nutrient-replete conditions ranges from approximately 20 in *L. fissa* to 60 in *A. minutum*.

The crude protein estimate appears to be an overestimate because the N content of protein derived from its average stoichiometry (0.16 g N/g protein) is larger than the PON measurement. To remove potentially absorbing substances that might bias the crude protein estimate we precipitated the crude protein extract. Precipitated protein is approximately 25 to 35% of the crude protein, increasing with nitrogen starvation (Fig. S2). Precipitated protein and the other nitrogen containing macromolecules measured do not account for all of total organic carbon or total organic nitrogen, indicating precipitated protein is significantly underestimating total protein content (Fig. S2), likely indicating incomplete protein extraction by the bead milling process. We focus our analysis on the crude protein for ease of comparison to the majority of these measurements in the literature.

Under resource-saturated exponential growth conditions, RNA:DNA and RNA:protein vary ~3-fold across the species; *P. triestinum* has the highest and *L. fissa* the lowest values of both ratios. In part this is because *P. triestinum* has the smallest and *L. fissa* the largest genome and in part this is due to RNA:PON and RNA:protein being highest in *P. triestinum* and lowest in *L. fissa* (Fig. S3). N-starvation causes declines in RNA:DNA, RNA:PON and Protein:PON, but no significant change in RNA:protein (Fig. S3). DNA:PON increases because PON declines with N-starvation.

4. Discussion

Genome size varies by a factor of approximately 64,000 across the tree of life (Pellicer et al. 2010) but most eukaryotes have genome sizes less than 20 pg (Hidalgo et al. 2017). Dinoflagellate DNA content ranges from 1.5 to 850 pg (Hong et al. 2016; LaJeunesse et al. 2005; Liu et al. 2021). The smallest dinoflagellate genomes are associated with *Symbiodinium,* a symbiont and small-sized dinoflagellate (LaJeunesse et al. 2005) but see Lin (2006). Larger dinoflagellate genomes are generally associated with species with larger cell volumes and often have high gene copy numbers (Liu et al. 2021). The DNA content of the dinoflagellates examined here, *P. triestinum* (14.8 ± 1.1), *A. minutum* (32.2 ± 4.7, mean ± sd), and *L. fissa* (184 ± 31 pg DNA), increase with cell volume and cellular carbon content (Table S1, Fig. 2). Compared to the diatoms *Thalassiosira pseudonana* and *T. weissflogii* these dinoflagellates are >3-fold higher in DNA:C and DNA:N and lower in RNA:DNA under resource-saturating exponential growth conditions (Fig. 3). These

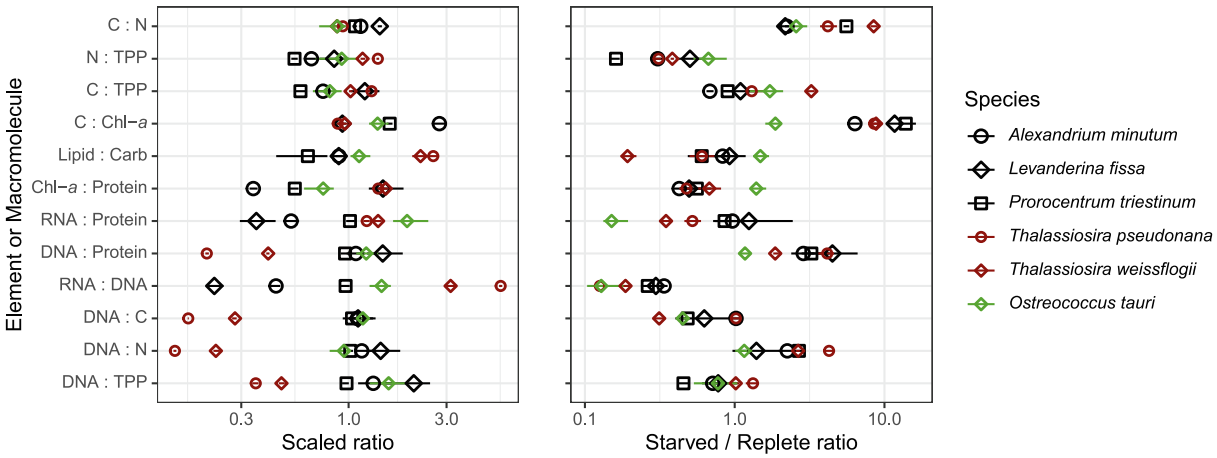

Fig. 3. Comparison of the elemental (mol:mol) and macromolecular composition (wt:wt) of dinoflagellates (this study) to the diatoms T. pseudonana and T. weisflogii and green photosynthetic picoeukaryote O. tauri (from Liefer et al. 2019). Ratios under replete conditions (left panel) shown scaled by the median ratio across all taxa to facilitate comparison of the variation across taxa and ratios. Ratios under N-starved conditions relative to replete conditions (right panel) highlight the differential effects of N-starvation across taxa and ratios. N-starved data are from mid-stationary phase, 9–11 days after onset of the N-starvation treatment. Both ratios shown on log scales with error bars showing 95% CI on geometric mean of replicates.

results are largely consistent with the genome streamlining hypothesis (Hessen et al. 2010): selection for smaller genomes and higher RNA:DNA for fast growth under resource-limiting conditions. Diatoms typically have both higher maximum growth rates and higher Chl-*a*:C than dinoflagellates of similar size (Tang 1996). *P. triestinum*, a photoautotrophic dinoflagellate (Lin 2011), is an anomaly in this regard, with a similar maximum growth rate and cell volume as the diatom *Thalassiosira weissflogii* (Liefer et al. 2019).

Total DNA content relative to total cellular C, N and P in dinoflagellates is comparable to the smallest known photosynthetic picoeukaryote, the green phytoplankter *Ostreococcus*. *Ostreococcus tauri* has a cell diameter of approximately 1 μm (Courties et al. 1994). Assuming there is a minimum viable size for a eukaryotic genome (as a non-scalable component), Raven (1986) hypothesized that the nucleus will take up a larger and more substantive proportion of the total mass of eukaryotes smaller than 3 μm in diameter. Other slightly larger photosynthethic picoeukaryotes such as the diploid Chloropicophyceae have similarly high DNA to carbon ratios to *Ostreococcus* (Ebenezer et al. 2022) and the dinoflagellates examined here. Under resource-saturating exponential growth conditions, RNA:DNA in *Ostreococcus* and the Chloropicophyceae are intermediate to the relatively low values in the dinoflagellates and higher values in the diatoms (Fig. 3). Cell size, genome size and associated ribosomal content, will influence cellular N and P requirements, and may constrain growth rate and macromolecular composition of these different eukaryotes in nitrogen- and phosphorus-limited regimes (Hessen et al. 2010).

Marine planktonic photosynthetic dinoflagellate C:N:P from resource-saturated lab cultures in exponential growth indicate that dinoflagellates tend to be higher in C:N (7.2 mol:mol) and lower in C:P (90.3) and N:P (11.5) than particulate matter in the surface ocean (Carnicer et al. 2021). The high C:N of dinoflagellates has been attributed to the dinoflagellate cell wall and amphisema, with thecate and smaller-sized (with their higher surface area to volume ratios) species tending to have higher carbohydrate content and higher C:N than athecate and larger species (Carnicer et al. 2021; Menden-Deuer and Lessard 2000). While the species examined here are also high in C:N (Fig. 3, Table S2), the large athecate species *L. fissa* Genomic architecture constrains macromolecular allocation in dinoflagellates (Kwok et al., 2023). It has been assumed that the typically low values of C:P and N:P in dinoflagellates was due to their large genome size and perhaps stores of polyphosphate (Carnicer et al. 2021). For the dinoflagellates examined here, under resource saturating growth conditions, DNA accounts for between 13% and 23% and RNA accounts for 6 to 17% of intracellular phosphorus – with the highest values being associated with the largest dinoflagellate examined, *L. fissa*. *L. fissa* with its high DNA content has a relatively high C:P and N:P compared to the smaller-sized *A. minutum* and *P. triestinum* (Figs 2, 3); this result highlights that storage P, as well as DNA and RNA, contribute to cellular P (Figs 2 and 3) and the low C:P and N:P of dinoflagellates. The production of C- rich and N-rich toxins, such as paralytic shellfish poisoning (PSP), can also influence the elemental stoichiometry of the cells (Carnicer et al. 2021). Some strains of *Alexandrium minutum* can produce PSP (Anderson et al. 2012); we suspect the strain used in this study is non-toxic as nitrogen content in *A. minutum* is not particularly high compared to the other species examined.

Hidalgo et al. (2017) have speculated that 150 Gb (~150 pg) may be approaching the maximum possible genome size. Larger genomes have high nutrient demand and additional biochemical and energy requirements that can impact cell division rate (Hessen et al. 2010) and have additional knock-on consequences for nutrient demand. For example, DNA damage and replication will scale with genome size; DNA repair requires ATP and investment in nitrogen-rich repair machinery and larger genomes may contribute to cell division rates (Hidalgo et al. 2017). Larger genomes are often associated with larger cell sizes (Shuter et al. 1983) which have higher nutrient requirements (per cell) (Shuter 1978), lower nutrient and gas diffusion rates, and lower growth rates (Finkel et al. 2010). Larger genomes are often associated with large gene islands separated by long repetitive non-coding regions, that can become highly condensed chromatin that may reduce the probability of genome downsizing events (Hidalgo et al. 2017). Over the long-term this may reduce gene expression and the ability of organisms to effectively respond to change. Although Hidalgo et al. (2017) have questioned whether the large genome sizes reported for dinoflagellates may be technical artifacts, dinoflagellates genomes exhibit several of the genetic characteristics they propose would result from large genomes: their DNA is permanently condensed without nucleosomes (Rizzo and Nooden 1973), their genes are organized in tandem repeats and many genes have high copy numbers (Liu et al. 2021), and there is some suggestion that they have relatively limited transcriptional regulation, that may influence their responsiveness to environmental perturbations.

There is scattered evidence that dinoflagellates may be less physiological and biochemically responsive to environmental stressors than other phytoplankton such as diatoms. For example, in response to a wide range of irradiances and growth rates, cell volume, protein, carbohydrate, and RNA content per cell remains constant in *Amphidinium carteri* (Thomas and Carr 1985). Phosphorus deficiency stimulates only minor

changes to N:P in a variety of dinoflagellates, and nitrogen limitation caused little change in the ratio of protein to carbohydrate in *A. carteri* (Sakshaug 1973; Sakshaug et al. 1984). Nitrogen deficiency had only minor impacts on the PSII quantum yield of photochemistry (Fv:Fm) in *Karenia mikimotoi* and *Prorocentrum shikokuense* (H. Li et al. 2021; Shi et al. 2021), and in *Lingulodinium polyedrum* it took almost a week in N-depleted conditions to observed a decline in photosynthetic carbon fixation (Dagenais Bellefeuille et al., 2014). In contrast, a typical response of many eukaryotic phytoplankton (diatoms and greens) to N-starvation is a substantive decline in photosynthetic efficiency (Z. Li et al. 2021; Liefer et al. 2018), and as seen in the dinoflagellates in this study (Fig. S1), a sharp decrease in cellular nitrogen content and N-containing macromolecules such as protein and chlorophyll, and decreases in RNA:protein, that all contribute to a decline in N:P. In diatoms and green algae there is also usually an accumulation of carbohydrate and then lipid stores with N-starvation, resulting in an increase in particulate carbon content and C:N (Ebenezer et al. 2022; Liefer et al. 2019; Sakshaug and Holm-Hansen 1977). Across a range of eukaryotic phytoplankton groups, nitrogen starvation often has only a minor impact on total phosphorus content (Ebenezer et al. 2022; Liefer et al. 2019; Sakshaug and Holm-Hansen 1977). Here we confirm that dinoflagellates have a somewhat atypical biochemical response to nitrogen starvation: cellular phosphorus accumulates in *P. triestinum* and *A. minutum* as has been reported for several other dinoflagellate species (see Qi et al. 2013; Smalley et al. 2003; Vidyarathna and Granéli 2013 for other examples), likely due to the accumulation of phosphate stores and a relatively moderated reduction in RNA content, resulting in atypically large decreases in N:P. Cellular lipid, carbohydrate, and POC changed relatively little with N-starvation, except in *P. triestinum* which increased in both lipid and carbohydrate resulting in an increase in total cellular carbon, perhaps because it is strictly photoautotrophic (Lin 2011). Under many conditions, across a large range of organisms, RNA content and RNA:protein increases with growth rate (Elser et al. 2003). In the dinoflagellates examined here, RNA:protein does not decline with the reduction and eventual cessation of cell division associated with nitrogen starvation, but is instead low and relatively invariant (Fig. S3, note RNA/PON and protein/PON show similar decreases over time in N-deplete media for all three dinoflagellate species) in constrast to diatoms and a range of green phytoplankton species examined (Fig. 3, Ebenezer et al. 2022; Liefer et al. 2019). These results reveal a unique linkage between total protein and ribosome content in dinoflagellates that may explain why N:P does not decrease with phosphorus deficiency when phosphorus stores are relatively depleted (Sakshaug et al. 1984).

The large genomes and phosphate content of dinoflagellates make them low in N:P compared to many other phytoplankton groups. Under nitrogen starvation and phosphate sufficiency dinoflagellates become even lower in N:P relative to other eukaryotes through an accumulation of phosphorus and invariance in RNA:protein. Polyphosphate is commonly synthesized by bacteria, including cyanobacteria, in response to stressful conditions, including nutrient starvation (Rao et al. 2009; Sanz-Luque et al. 2020). In contrast, many eukaryotic phytoplankton species do not increase in phosphorus content in response to nitrogen starvation (Fig. 3, but see Chu et al. (2020)). *Prorocentrum donghaiense* has been shown to store phosphate as intracellular polyphosphate (S.-F. Zhang et al. 2019). Polyphosphate may have numerous cellular functions: as a phosphate or chemical bond energy store that can be advantageous in pulsed environments (Kornberg 1995), as a P reservoir to assist in maintaining cellular P homeostasis, and playing an important regulatory role in the cell division cycle, growth rate, and metabolism (Bru et al. 2016; Rao et al. 2009; Sanz-Luque et al. 2020). In the bacteria, *Pseudomonas aeruginosa* polyphosphate has been associated with successful cell cycle exit and nucleoid compaction under nitrogen starvation, and in *E. coli* polyphosphate has been linked with DNA-specific binding of the nucleoid-associated silencing factor HFq and associated heterochromatin formation and decreases in mutagenesis rates and DNA damage-induced cell death (Beaufay et al. 2021; Magkiriadou et al. 2021; Racki et al. 2017). Based on these observations, we speculate that phosphate stores may play an important role in supporting the unique structure and high phosphorus requirements of dinoflagellate genomes, but more research is required to determine the role nutrient starvation and phosphate stores plays in dinoflagellate metabolism, ecology and evolution.

CRediT authorship contribution statement

Olga Carnicer: Conceptualization, Investigation, Writing – original draft, Writing – review & editing. **Ying-Yu Hu:** Methodology, Validation, Writing – original draft, Writing – review & editing. **Vinitha Ebenezer:** Investigation. **Andrew J. Irwin:** Formal analysis, Data curation, Visualization, Funding acquisition, Supervision, Writing – original draft, Writing – review & editing. **Zoe V. Finkel:** Conceptualization, Formal analysis, Project administration, Funding acquisition, Supervision, Writing – original draft, Writing – review & editing.

Declaration of Competing Interest

The authors declare that they have no known competing financial interests or personal relationships that could have appeared to influence the work reported in this paper.

Data availability

Data are provided in the supplementary materials

Acknowledgements

We thank Doug Wallace, Claire Normandeau and Dalhousie Oceanography for assistance with CHN and dissolved nutrient analyses, and Khadijah Carey and Gracie Walker for their assistance with sample collection and cell volume analyses. We thank Margarita Fernández-Tejedor and Maria Rey for providing us with *A. minutum* strain. This work was supported by the Simons Collaboration on Computational Biogeochemical Modeling of Marine Ecosystems (CBIOMES, grant 549935 (AJI) and 549937 (ZVF), Simons Collaboration on Ocean Processes and Ecology (Gradients, grant 723789 (ZVF) and 721235 (AJI)), the Canada Research Chairs program, and NSERC.

Appendix A. Supplementary material

Supplementary data to this article can be found online at https://doi.org/10.1016/j.protis.2023.125992.

References

Anderson, D.M., Alpermann, T.J., Cembella, A.D., Collos, Y., Masseret, E., Montresor, M., 2012. The globally distributed genus *Alexandrium*: Multifaceted roles in marine ecosystems and impacts on human health. Harmful Algae 14, 10–35.

Anderson, D.M., Garrison, D.J., 1997. Ecology and oceanography of harmful algal blooms. Limnol Oceanogr 42, 1009–1305.

Beauchemin, M., Roy, S., Daoust, P., Dagenais-Bellefeuille, S., Bertomeu, T., Letourneau, L., Lang, B.F., Morse, D., 2012. Dinoflagellate tandem array gene transcripts are highly conserved and not polycistronic. Proc Natl Acad Sci 109 (39), 15793–15798.

Beaufay, F., Amemiya, H.M., Guan, J., Basalla, J., Meinen, B.A., Chen, Z., Mitra, R., Bardwell, J.C., Biteen, J.S., Vecchiarelli, A.G., 2021. Polyphosphate drives bacterial heterochromatin formation. Sci Adv 7 (52), eabk0233.

Béchemin, C., Grzebyk, D., Hachame, F., Hummert, C., Maestrini, S.Y., 1999. Effect of different nitrogen/phosphorus nutrient ratios on the toxin content in *Alexandrium minutum*. Aquat Microb Ecol 20 (2), 157–165. https://doi.org/10.3354/ame020157.

Berdalet, E., Roldán, C., Olivar, M.P., 2005. Quantifying RNA and DNA in planktonic organisms with SYBR Green II and nucleases. Part B. Quantification in natural samples. Sci Marina 69, 17–30. https://doi.org/10.3989/scimar.2005.69n117.

Bru, S., Martínez-Laínez, J.M., Hernández-Ortega, S., Quandt, E., Torres-Torronteras, J., Marti, R., Canadell, D., Arino, J., Sharma, S., Jiménez, J., 2016. Polyphosphate is involved in cell cycle progression and genomic stability in *Saccharomyces cerevisiae*. Mol Microbiol 101 (3), 367–380.

Carnicer, O., Irwin, A.J., Finkel, Z.V., 2021. Traits influence dinoflagellate C:N:P. Eur J Phycol 57, 154–165. https://doi.org/10.1080/09670262.2021.1914860.

Chu, F., Cheng, J., Li, K., Wang, Y., Li, X., Yang, W., 2020. Enhanced lipid accumulation through a regulated metabolic pathway of phosphorus luxury uptake in the microalga *Chlorella vulgaris* under nitrogen starvation and phosphorus repletion. ACS Sustain Chem Eng 8 (22), 8137–8147.

Courties, C., Vaquer, A., Trousselier, M., Lautier, J., Chrétiennot-Dinet, M.J., Neveux, J., Machado, C., Claustre, H., 1994. Smallest eukaryotic organism. Nature 370, 255.

Dagenais Bellefeuille, S., Dorion, S., Rivoal, J., Morse, D., 2014. The dinoflagellate Lingulodinium polyedrum responds to N depletion by a polarized deposition of starch and lipid bodies. PLoS One 9 (11), e111067.

Deutsch, C., Weber, T., 2012. Nutrient ratios as a tracer and driver of ocean biogeochemistry. Ann Rev Mar Sci 4 (1), 113–141. https://doi.org/10.1146/annurev-marine-120709-142821.

Ebenezer, V., Hu, Y., Carnicer, O., Irwin, A.J., Follows, M.J., Finkel, Z.V., 2022. Elemental and macromolecular composition of the marine Chloropicophyceae, a major group of oceanic photosynthetic picoeukaryotes. Limnol Oceanogr 67 (3), 540–551.

Eker-Develi, E., Kideys, A.E., Tugrul, S., 2006. Effect of nutrients on culture dynamics of marine phytoplankton. Aquat Sci 68 (1), 28–39. https://doi.org/10.1007/s00027-005-0810-5.

Elser, J.J., Acharya, K., Kyle, M., Cotner, J., Makino, W., Markow, T., Watts, T., Hobbie, S., Fagan, W., Schade, J., Hood, J., Sterner, R.W., 2003. Growth rate-stoichiometry couplings in diverse biota. Ecol Lett 6, 936–943.

Finkel, Z.V., Beardall, J., Flynn, K., Quigg, A.S., Rees, T.A.V., Raven, J.A., 2010. Phytoplankton in a changing world: Cell size and elemental stoichiometry. J Plankton Res 32 (1), 119–137.

Flynn, K., Jones, K.J., Flynn, K.J., 1996. Comparisons among species of *Alexandrium* (Dinophyceae) grown in nitrogen- or phosphorus-limiting batch culture. Mar Biol 126 (1), 9–18. https://doi.org/10.1007/BF00571372.

Geider, R.J., LaRoche, J., 2002. Redfield revisited: Variability of C:N: P in marine microalgae and its biochemical basis. Eur J Phycol 37, 1–17.

Gómez, F., 2012. A checklist and classification of living dinoflagellates (Dinoflagellata, Alveolata). Cicimar Oceánides 27 (1), 65–140.

Hackett, J.D., Bhattacharya, D., 2006. The genomes of dinoflagellates. In: Genomics and evolution of microbial eukaryotes. Oxford University Press, New York, pp. 48–63.

Hallegraeff, G.M., 1993. A review of harmful algal blooms and their apparent global increase. Phycologia 32 (2), 79–99.

Herzog, M., Soyer, M., Daney de Marcillac, G., 1982. A high level of thymine replacement by 5-hydroxymethyluracil in nuclear DNA of the primitive dinoflagellate *Prorocentrum micans* E. Eur J Cell Biol 27 (2), 151–155.

Hessen, D.O., Jeyasingh, P.D., Neiman, M., Weider, L.J., 2010. Genome streamlining and the elemental costs of growth. Trends Ecol Evol 25 (2), 75–80.

Hidalgo, O., Pellicer, J., Christenhusz, M., Schneider, H., Leitch, A.R., Leitch, I.J., 2017. Is there an upper limit to genome size? Trends Plant Sci 22 (7), 567–573.

Hong, H.-H., Lee, H.-G., Jo, J., Kim, H.M., Kim, S.-M., Park, J.Y., Jeon, C.B., Kang, H.-S., Park, M.G., Park, C., 2016. The exceptionally large genome of the harmful red tide dinoflagellate *Cochlodinium polykrikoides* Margalef (Dinophyceae): Determination by flow cytometry. Algae 31 (4), 373–378.

Hoppenrath, M., 2017. Dinoflagellate taxonomy—A review and proposal of a revised classification. Mar Biodivers 47 (2), 381–403.

Hu, Y.-Y., Finkel, Z.V., 2022a. Lipids in microalgae: Quantitation by acid-dichromate method in microtiter plate. Protocols.Io. https://doi.org/10.17504/protocols.io.e6nvw9dpzgmk/v2.

Hu, Y.-Y., Finkel, Z.V., 2022b. Rapid extraction of total lipids from microalgae. Protocols.Io. https://doi.org/10.17504/protocols.io.dm6gpr9jdvzp/v5.

Hu, Y.-Y., Finkel, Z.V., 2022c. Total particulate carbohydrate from microalgae. Protocols.Io. https://doi.org/10.17504/protocols.io.yxmvmk24ng3p/v1.

Hu, Y.-Y., Irwin, A.J., Finkel, Z.V., 2022. Improving quantification of particulate phosphorus. Limnol Oceanogr Methods 20 (11), 729–740.

Hu, Y.-Y., Lord, C., Finkel, Z.V., 2022a. Chloroform-methanol protein precipitation from microalgae and Pierce BCA assay. Protocols.Io. https://doi.org/10.17504/protocols.io.yxmvm2e25g3p/v1.

Hu, Y.-Y., Lord, C., Finkel, Z.V., 2022b. Total crude protein in plankton: Pierce BCA protein assay (including the enhanced assay for low biomass). Protocols.Io. https://doi.org/10.17504/protocols.io.5qpvoy5e7g4o/v3.

Irwin, A.J., Nelles, A.M., Finkel, Z.V., 2012. Phytoplankton niches estimated from field data. Limnol Oceanogr 57 (3), 787–797.

John, E.H., Flynn, K.J., 2000. Growth dynamics and toxicity of *Alexandrium fundyense* (Dinophyceae): The effect of changing N: P supply ratios on internal toxin and nutrient levels. Eur J Phycol 35 (1), 11–23. https://doi.org/10.1080/09670260010001735581.

Kornberg, A., 1995. Inorganic polyphosphate: Toward making a forgotten polymer unforgettable. J Bacteriol 177 (3), 491–496.

Kwok, A.C.M., Chan, W.S., Wong, J.T.Y., 2023. Dinoflagellate amphiesmal dynamics: Cell wall deposition with ecdysis and cellular growth. Mar Drug 21 (2), 70.

LaJeunesse, T.C., Lambert, G., Andersen, R.A., Coffroth, M.A., Galbraith, D.W., 2005. Symbiodinium (Pyrrhophyta) genome sizes (DNA content) are smallest among dinoflagellates. J Phycol 41 (4), 880–886.

Leterme, S.C., Edwards, M., Seuront, L., Attrill, M.J., Reid, P.C., John, A.W.G., 2005. Decadal basin-scale changes in diatoms, dinoflagellates, and phytoplankton colour in the North Atlantic. Limnol Oceanogr 50 (4), 1244–1253.

Li, H., Li, L., Yu, L., Yang, X., Shi, X., Wang, J., Li, J., Lin, S., 2021a. Transcriptome profiling reveals versatile dissolved organic nitrogen utilization, mixotrophy, and N conservation in the dinoflagellate *Prorocentrum shikokuense* under N deficiency. Sci Total Environ 763, 143013.

Li, Z., Li, W., Zhang, Y., Hu, Y., Sheward, R., Irwin, A.J., Finkel, Z.V., 2021b. Dynamic photophysiological stress response of a model diatom to ten environmental stresses. J Phycol 57 (2), 484–495. https://doi.org/10.1111/jpy.13072.

Liefer, J.D., Garg, A., Campbell, D.A., Irwin, A.J., Finkel, Z.V., 2018. Nitrogen starvation induces distinct photosynthetic responses and recovery dynamics in diatoms and prasinophytes. PLoS One 13 (4), e0195705.

Liefer, J.D., Garg, A., Fyfe, M.H., Irwin, A.J., Benner, I., Brown, C.M., Follows, M.J., Omta, A.W., Finkel, Z.V., 2019. The macromolecular basis of phytoplankton C: N: P under nitrogen starvation. Front Microbiol 10, 763.

Lin, S., 2006. The smallest dinoflagellate genome is yet to be found: A comment on LaJeunesse et al. "*Symbiodinium* (Pyrrhophyta) genome sizes (DNA content) are smallest among dinoflagellates". J Phycol 42 (3), 746–748.

Lin, S., 2011. Genomic understanding of dinoflagellates. Res Microbiol 162 (6), 551–569.

Liu, Y., Hu, Z., Deng, Y., Shang, L., Gobler, C.J., Tang, Y.Z., 2021. Dependence of genome size and copy number of rRNA gene on cell volume in dinoflagellates. Harmful Algae 109, 102108.

Livolant, F., Bouligand, Y., 1978. New observations on the twisted arrangement of dinoflagellate chromosomes. Chromosoma 68 (1), 21–44.

Magkiriadou, S., Habel, A., Stepp, W., Newman, D., Manley, S., Racki, L., 2021. Polyphosphate affects cytoplasmic and chromosomal dynamics in nitrogen-starved *Pseudomonas aeruginosa*. BioRxiv 2021–2112. https://doi.org/10.1101/2021.12.23.473106.

Marinov, G.K., Trevino, A.E., Xiang, T., Kundaje, A., Grossman, A.R., Greenleaf, W.J., 2021. Transcription-dependent domain-scale three-dimensional genome organization in the dinoflagellate *Breviolum minutum*. Nat Genet 53 (5), 613–617.

Menden-Deuer, S., Lessard, E.J., 2000. Carbon to volume relationships for dinoflagellates, diatoms, and other protist plankton. Limnol Oceanogr 45, 569–579.

Myklestad, S.M., Skånøy, E., Hestmann, S., 1997. A sensitive and rapid method for analysis of dissolved mono-and polysaccharides in seawater. Mar Chem 56 (3–4), 279–286.

Ni, G., Zimbalatti, G., Murphy, C.D., Barnett, A.B., Arsenault, C.M., Li, G., Cockshutt, A. M., Campbell, D.A., 2017. Arctic *Micromonas* uses protein pools and non-photochemical quenching to cope with temperature restrictions on Photosystem II protein turnover. Photosynth Res 131, 203–220.

Ou, L., Huang, K., Li, J.-J., Jing, W.-Y., Dong, H.-P., 2019. Transcriptomic responses of harmful dinoflagellate *Prorocentrum donghaiense* to nitrogen and light. Mar Pollut Bull 149, 110617.

Pande, S., Khan, R.P., Venkitasubramanian, T., 1963. Microdetermination of lipids and serum total fatty acids. Anal Biochem 6 (5), 415–423.

Pellicer, J., Fay, M.F., Leitch, I.J., 2010. The largest eukaryotic genome of them all? Bot J Linn Soc 164 (1), 10–15.

Qi, H., Wang, J., Wang, Z., 2013. A comparative study of maximal quantum yield of photosystem II to determine nitrogen and phosphorus limitation on two marine algae. J Sea Res 80, 1–11. https://doi.org/10.1016/j.seares.2013.02.007.

Racki, L.R., Tocheva, E.I., Dieterle, M.G., Sullivan, M.C., Jensen, G.J., Newman, D.K., 2017. Polyphosphate granule biogenesis is temporally and functionally tied to cell cycle exit during starvation in *Pseudomonas aeruginosa*. Proc Nat Acad Sci 114 (12), E2440–E2449.

Rae, P.M., 1976. Hydroxymethyluracil in eukaryote DNA: a natural feature of the Pyrrophyta (dinoflagellates). Science 194 (4269), 1062–1064.

Rao, N.N., Gómez-García, M.R., Kornberg, A., 2009. Inorganic polyphosphate: Essential for growth and survival. Annu Rev Biochem 78, 605–647.

Raven, J.A., 1986. Physiological consequences of extremely small size for autotrophic organisms in the sea. In: Platt, T.R., Li, W.K.W. (Eds.), Photosynthetic picoplankton, vol. 214, pp. 1–70.

Rizzo, P.J., 2003. Those amazing dinoflagellate chromosomes. Cell Res 13 (4), 215–217.

Rizzo, P.J., Nooden, L.D., 1973. Isolation and chemical composition of dinoflagellate nuclei. J Protozool 20 (5), 666–672.

Sakshaug, E., 1973. Production of protein and carbohydrate in the dinoflagellate *Amphidinium carteri*. Some preliminary results. Nor J Bot 20, 211–218.

Sakshaug, E., Granéli, E., Elbrächter, M., Kayser, H., 1984. Chemical composition and alkaline phosphatase activity of nutrient-saturated and P-deficient cells of four marine dinoflagellates. J Exp Mar Biol Ecol 77 (3), 241–254.

Sakshaug, E., Holm-Hansen, O., 1977. Chemical composition of Skeletonema costatum (Grev.) Cleve and Pavlova (Monochrysis) lutheri (Droop) Green as a function of nitrate-, phosphate-, and iron-limited growth. J Exp Mar Biol Ecol 29 (1), 1–34.

Sanz-Luque, E., Bhaya, D., Grossman, A.R., 2020. Polyphosphate: A multifunctional metabolite in cyanobacteria and algae. Front Plant Sci 11, 938.

Shi, X., Xiao, Y., Liu, L., Xie, Y., Ma, R., Chen, J., 2021. Transcriptome responses of the dinoflagellate Karenia mikimotoi driven by nitrogen deficiency. Harmful Algae 103, 101977.

Shumway, S.E., 1990. A review of the effects of algal blooms on shellfish and aquaculture. J World Aquacult Soc 21 (2), 65–104.

Shuter, B.J., 1978. Size dependence of phophorus and nitrogen subsistence quotas in unicellular microrganisms. Limnol Oceanogr 23 (6), 1248–1255.

Shuter, B.J., Thomas, J.E., Taylor, W.D., Zimmerman, A.M., 1983. Phenotypic correlates of genocmic DNA content in unicellular eukaryotes and other cells. Am Nat 122 (1), 26–44.

Smalley, G.W., Coats, D.W., Stoecker, D.K., 2003. Feeding in the mixotrophic dinoflagellate Ceratium furca is influenced by intracellular nutrient concentrations. Mar Ecol Prog Ser 262, 137–151. https://doi.org/10.3354/meps262137.

Smayda, T.J., Reynolds, C.S., 2003. Strategies of marine dinoflagellate survival and some rules of assembly. J Sea Res 49 (2), 95–106.

Solórzano, L., Sharp, J.H., 1980. Determination of total dissolved phosphorus and particulate phosphorus in natural waters1. Limnol Oceanogr 25 (4), 754–758. https://doi.org/10.4319/lo.1980.25.4.0754.

Spector, D.L., 1984. Dinoflagellate nuclei. Dinoflagellates 1, 107–147.
Sterner, R.W., Elser, J.J., 2002. Ecological stoichiometry: The biology of the elements from molecules to the biosphere. Princeton University Press.
Tang, E.P.Y., 1996. Why do dinoflagellates have lower growth rates? J Phycol 32 (1), 80–84.
Thomas, P.H., Carr, N.G., 1985. The invariance of macromolecular composition with altered light limited growth rate of Amphidinium carteri (Dinophyceae). Arch Microbiol 142, 81–86.
Tovar-Sanchez, A., Sañudo-Wilhelmy, S.A., Garcia-Vargas, M., Weaver, R.S., Popels, L.C., Hutchins, D.A., 2003. A trace metal clean reagent to remove surface-bound iron from marine phytoplankton. Mar Chem 82 (1), 91–99. https://doi.org/10.1016/S0304-4203(03)00054-9.
Vidyarathna, N.K., Granéli, E., 2013. Physiological responses of Ostreopsis ovata to changes in N and P availability and temperature increase. Harmful Algae 21–22, 54–63. https://doi.org/10.1016/j.hal.2012.11.006.
Williams, R.G., Follows, M.J., 2011. Ocean dynamics and the carbon cycle: Principles and mechanisms. Cambridge University Press.
Zhang, H., Hou, Y., Miranda, L., Campbell, D.A., Sturm, N.R., Gaasterland, T., Lin, S., 2007. Spliced leader RNA trans-splicing in dinoflagellates. Proc Natl Acad Sci 104 (11), 4618–4623.
Zhang, H., Campbell, D.A., Sturm, N.R., Lin, S., 2009. Dinoflagellate spliced leader RNA genes display a variety of sequences and genomic arrangements. Mol Biol Evol 26 (8), 1757–1771.
Zhang, S.-F., Yuan, C.-J., Chen, Y., Lin, L., Wang, D.-Z., 2019. Transcriptomic response to changing ambient phosphorus in the marine dinoflagellate *Prorocentrum donghaiense*. Sci Total Environ 692, 1037–1047.